The Earth atmosphere-like bulk nitrogen isotope composition obtained by stepwise combustion analyses of Ryugu return samples

Author(s):
Hashizume, Ko; Ishida, Akizumi; Chiba, Ayano; Okazaki, Ryuji; Yogata, Kasumi; Yada, Toru; Kitajima, Fumio; Yurimoto, Hisayoshi; Nakamura, Tomoki; Noguchi, Takaaki; Yabuta, Hikaru; Naraoka, Hiroshi; Takano, Yoshinori; Sakamoto, Kanako; Tachibana, Shogo; Nishimura, Masahiro; Nakato, Aiko; Miyazaki, Akiko; Abe, Masanao; Okada, Tatsuaki; Busemann, Henner; et al.

Publication date:
2024-08

Permanent link:
https://doi.org/https://doi.org/10.3929/ethz-b-000673030

Originally published in:
Meteoritics & Planetary Science 59(8), https://doi.org/10.1111/maps.14175

The Meteoritical Society

Meteoritics & Planetary Science 59, Nr 8, 2117–2133 (2024)
doi: 10.1111/maps.14175

The Earth atmosphere-like bulk nitrogen isotope composition obtained by stepwise combustion analyses of Ryugu return samples

Ko HASHIZUME[1,*], Akizumi ISHIDA[2], Ayano CHIBA[1], Ryuji OKAZAKI[3], Kasumi YOGATA[4], Toru YADA[4], Fumio KITAJIMA[3], Hisayoshi YURIMOTO[5], Tomoki NAKAMURA[2], Takaaki NOGUCHI[6], Hikaru YABUTA[7], Hiroshi NARAOKA[3], Yoshinori TAKANO[8], Kanako SAKAMOTO[4], Shogo TACHIBANA[9], Masahiro NISHIMURA[4], Aiko NAKATO[4], Akiko MIYAZAKI[4], Masanao ABE[4], Tatsuaki OKADA[4], Tomohiro USUI[4], Makoto YOSHIKAWA[4], Takanao SAIKI[4], Fuyuto TERUI[10], Satoshi TANAKA[4], Satoru NAKAZAWA[4], Sei-ichiro WATANABE[11], Yuichi TSUDA[4], Michael W. BROADLEY[12], Henner BUSEMANN[13], and the Hayabusa2 Initial Analysis Volatile Team

[1]Faculty of Science, Ibaraki University, Mito, Japan
[2]Department of Earth Science, Tohoku University, Sendai, Japan
[3]Department of Earth and Planetary Sciences, Kyushu University, Fukuoka, Japan
[4]Institute of Space and Astronautical Science, Japan Aerospace Exploration Agency (JAXA), Sagamihara, Japan
[5]Department of Earth and Planetary Sciences, Hokkaido University, Sapporo, Japan
[6]Division of Earth and Planetary Sciences, Kyoto University, Kyoto, Japan
[7]Department of Earth and Planetary Systems Science, Hiroshima University, Higashi-Hiroshima, Japan
[8]Biogeochemistry Research Center, Japan Agency for Marine-Earth Science and Technology, Yokosuka, Japan
[9]UTokyo Organization for Planetary and Space Science, The University of Tokyo, Tokyo, Japan
[10]Kanagawa Institute of Technology, Atsugi, Japan
[11]Department of Earth and Environmental Sciences, Nagoya University, Nagoya, Japan
[12]CRPG, CNRS, Université de Lorraine, Vandoeuvre-lès-Nancy, France
[13]Institute of Geochemistry and Petrology, ETH Zürich, Zürich, Switzerland

***Correspondence**
Ko Hashizume, Faculty of Science, Ibaraki University, Mito 310-8512, Japan.
Email: ko.hashizume.sci@vc.ibaraki.ac.jp

(Received 09 April 2023; revision accepted 11 April 2024)

Abstract–The nitrogen isotope compositions of two samples returned from the asteroid Ryugu were determined using a stepwise combustion method, along with Ivuna (CI) and Y-980115, a CI-like Antarctic meteorite, as references. The two Ryugu samples A0105-07 and C0106-07 showed bulk $\delta^{15}N$ values of $+1.7 \pm 0.5‰$ and $+0.2 \pm 0.6‰$, respectively, significantly lower than Ivuna with $+36.4 \pm 0.4‰$, but close to Y-980115 with $+4.0 \pm 0.3‰$. The Ryugu samples are further characterized by C/N and $^{36}Ar/N$ ratios up to 3.4× and 4.9× the value of Ivuna, respectively. Among all Ryugu samples and CI chondrites, a positive correlation was observed between nitrogen concentrations and $\delta^{15}N$ values, with samples with lower nitrogen concentrations exhibiting lower $\delta^{15}N$. This trend is explained by a two-component mixing model. One component is present at a constant abundance among all CI-related samples, with a $\delta^{15}N$ value around 0‰ or lower. The other varies in abundance between different samples, and exhibits a $\delta^{15}N$ value of $+56 \pm 4‰$. The first ^{15}N-poor endmember is seemingly tightly incorporated into a carbonaceous host phase, whereas the ^{15}N-rich endmember can be mobilized and decoupled from carbon, potentially because it is in the form of ammonia. Asteroid materials with volatile compositions that are similar to those reported here for the Ryugu samples are attractive candidates for the volatile sources among Earth's building blocks.

INTRODUCTION

Nitrogen isotopes are a powerful tool in cosmochemistry to decipher the origin and evolution of planetary materials. The nitrogen isotope ratio $^{15}N/^{14}N$, usually expressed by the delta notation, $\delta^{15}N \equiv [(^{15}N/^{14}N)/(^{15}N/^{14}N)_{AIR}-1] \times 1000$ (‰), exhibits large variations among different meteorites (Alexander et al., 2012; Füri & Marty, 2015; Hashizume, 2015; Kerridge, 1985; Marty, 2012; Pearson et al., 2006). The isotope ratio of nitrogen, being a typical volatile element, is particularly useful to constrain the formation and evolution processes of planetary atmospheres, including Earth and the other rocky planets. Viable Earth formation models assume that CI chondrite-like volatile-rich asteroids may have been one important volatile source to Earth (e.g., Alexander et al., 2012; Alexander, 2022; Budde et al., 2019; Dauphas, 2017; Marty, 2012), although not the primary source of rocky material that makes up the planet. Here, we pay attention to this type of potential Earth-forming building blocks, particularly with reference to the nitrogen isotope composition in a variety of planetary materials related to CI chondrites.

Three CI chondrite falls, Alais, Ivuna, and Orgueil, have been intensively studied so far for nitrogen isotopes. In this article, we collectively denote these meteorites as CI falls. CI falls exhibit fairly constant bulk $\delta^{15}N$ values typically around +40‰ (Alexander et al., 2012; Kerridge, 1985; Kung & Clayton, 1978; Robert & Epstein, 1982). As discussed later, the higher $\delta^{15}N$ values for the CI chondrites compared to the present Earth atmosphere impose important constraints on the formation and evolution history of the Earth atmosphere.

A recent search of the vast stock of Antarctic meteorites has revealed that there exist several Antarctic meteorites that share similar textures and mineralogical compositions with the CI falls. Though similar, these potential CI Antarctic meteorites still exhibit marked differences from the CI falls, particularly from a volatile element point of view. The majority of phyllosilicates are dehydrated in these Antarctic CI meteorites, while the phyllosilicates of CI falls mostly remain hydrated (King et al., 2019). Although these Antarctic meteorites are sometimes tentatively classified as "CY" chondrites (e.g., King et al., 2019), we treat them as being CI-related in our comparison with the Ryugu samples. The bulk $\delta^{15}N$ value for one of these Antarctic CI chondrites, Y-980115, was reported to be −2.8‰ (Chan et al., 2016), very different from those of the CI falls.

Here, we add another group of CI-related samples to be studied along with the abovementioned meteorites, the samples returned from the asteroid Ryugu. The textures and mineralogical compositions of the Ryugu samples have been reported to be similar with CI falls (Nakamura et al., 2022; Yokoyama et al., 2022). The abundances of hydrous minerals were found to be equivalent to those of the CI falls, although there has been partial loss of water that was weakly bound in minerals (Yokoyama et al., 2022). In this study, we examined, under the framework of the Hayabusa2 initial analysis campaign, the nitrogen abundances and isotope compositions of two Ryugu samples, with a view to investigating the large $\delta^{15}N$ difference observed between the hydrated CI falls and the dehydrated Antarctic CI chondrite. A subset of bulk compositional data for the Ryugu samples has been already published in a series of papers (Naraoka et al., 2023; Oba et al., 2023; Okazaki, Marty, et al., 2022). In this article, the full results of the stepwise combustion analyses performed on two Ryugu samples, A0105-07 and C0106-07, are reported. Using stepwise combustion, isotope ratios and volatile compositions from separate carrier phases that coexist in a bulk sample can be individually obtained and be resolved by their different respective combustion temperature. Readers are also referred to Broadley et al. (2023) for full sets of data for nitrogen and noble gas isotopes for another two Ryugu samples, A0105-05 and C0106-06.

SAMPLES AND METHODOLOGY

Sampling of Ryugu Grains

Samples were collected from the asteroid Ryugu during the two Hayabusa2 touchdown operations (Morota et al., 2020; Tachibana et al., 2022). During the first touchdown, samples that resided at the surface of the asteroid were collected, and stored in chamber A of the sample catcher. The second touchdown was done inside a 1.7 m-deep artificial crater (Arakawa et al., 2020), which was created by firing a 2 kg copper projectile at a velocity of ~2 km s^{-1} into the surface (Saiki et al., 2017). The samples acquired by this operation are expected to be a mixture of surface materials and those that have been located in the subsurface of the asteroid. The samples acquired by this operation were stored in chamber C. The sample names that start with A and C designate those collected by these two touchdown operations. The returned samples were handled and stored in a completely dry-nitrogen environment, and never came into contact with Earth's atmosphere (Yada et al., 2022).

Samples distributed to the volatile subteam were first pelletized (Okazaki, Yamanouchi, et al., 2022), then were analyzed by Fourier transform infrared spectroscopy (FT-IR), field-emission scanning electron microscopy, and energy dispersive x-ray spectroscopy (EDS) in a non-destructive manner. These procedures were also done in a dry-nitrogen environment (Okazaki, Marty, et al., 2022). The FT-IR analyses for the two samples A0105 and C0106, exhibit strong absorption by important functional groups (-OH, -NH, and -CH: see Figure S1). Based on the EDS analyses, modal abundances of Fe-sulfide and magnetite were estimated to be 1.9% and 6.9%, respectively, for A0105-07, and 2.0% and 5.7%, respectively, for C0106-07. These abundances fit within the typical ranges for Fe-sulfide ($3 \pm 1\%$) and magnetite ($5 \pm 2\%$) observed among eight Ryugu C samples, which further agree with the typical abundances of 1.1% and 4.3% found for Ivuna-type (CI) carbonaceous chondrites (Okazaki, Marty, et al., 2022). After these analyses, the samples were delivered to be prepared and installed into the gas source mass spectrometry line described below.

Analyses

At Tohoku University, samples A0105-07 and C0106-07 were individually wrapped in annealed platinum foils using a tool developed by Okazaki, Yamanouchi, et al. (2022). The wrapped samples were further sealed into aluminum containers. The wrapping and sealing procedures were performed in a glove box filled with dry nitrogen. The wrapped and sealed samples were then weighed using a micro balance (Mettler Toledo, XPR6UD). The samples were then transferred to Ibaraki University for nitrogen isotope analysis. Each sample wrapped in platinum was introduced into the vacuum line of the mass spectrometer system. This was done by placing the aluminum container, and the quartz combustion tube to be attached to the vacuum line, into an inflatable plastic glove box. Dry nitrogen constantly flowed through the bag during the insertion to avoid the sample coming into contact with the ambient atmosphere. The bulk Ivuna and Y-980115 samples were prepared for the analyses in a routine manner (e.g., Hashizume & Sugiura, 1995), washed with acetone, crushed, and wrapped in the platinum foil, under the ambient atmosphere. The quartz combustion tube was evacuated to vacuum, then was baked overnight at 1000°C. However, A0105-07, which was installed first, was baked for around a week at the same temperature. During the baking, the samples were stored in a branch, placed above the quartz combustion tube. They were heated to around 50°C by radiative heating from the combustion furnace.

For analysis, the sample was dropped into the quartz tube and was heated at designated temperatures in approximately 100 Pa of pure oxygen, by the stepwise combustion method. During combustion, the extracted gas was in contact with a platinum foil heated at 800°C to promote the transformation of miscellaneous gas compounds into N_2, and condensable molecules such as CO_2, H_2O, and SO_2. The condensable gases were removed by a cryogenic trap cooled by liquid nitrogen. The remaining oxygen was absorbed by CuO, with the remaining gas mainly consisting of nitrogen and noble gases. A fraction of gas, separated from the main part designated for nitrogen isotope analysis, was exposed to a Ti-Zr getter, to be subsequently analyzed for argon isotopes. The remaining gas was finally introduced into the mass spectrometer (BALZERS QMG420) operating in static mode for nitrogen isotope analysis. The amount of sample nitrogen to be introduced was adjusted to a level equivalent to about 1 pipette of standard N_2 gas (see below). This pressure adjustment was performed by dilution, evacuating a portion of the sample gas between the different volumes that make up the mass spectrometry line. The exact dependence of the measured isotope ratio on the nitrogen pressure was further corrected by previous analyses of different standard gas amounts (see Yamamoto et al., 1998). The carbon concentration was determined by measuring the pressure of the CO_2 released from the cryogenic trap using a crystal gauge, a hot-filament-free vacuum gauge (ANELVA M-320XG). This trap cooled at liquid nitrogen temperature traps the CO_2 gas, as well as other condensable gases, generated from the sample during combustion. Before the CO_2 pressure analysis, the CO_2 sample gas was separated from other condensable gases such as H_2O and SO_2 with a cool bath maintained at the melting temperature of 2-propanol (−69°C). The CO_2 sensitivity for the crystal gauge was calibrated by measuring combusted synthetic diamond with known impurity concentrations (Ishida et al., 2023).

Nitrogen impurities present in the oxygen introduced to the line at each combustion step, namely the cold-blank level, were estimated to be about 0.8 picomole of N_2. System blank levels of nitrogen, namely the hot-blank levels, vary with the combustion temperature, and with the number of past analyses performed using the same quartz tube. Normally, the blanks are as low as 0.2 picomole of N_2 at 800°C, rising to 30 picomole at 1200°C, for a combustion duration of 30 min, which is the standard duration applied for most of the combustion steps. Exceptions were the second 1200°C steps for C0106-07 and Ivuna, which lasted 120 min with the aim to totally release the remaining gas from the samples. The temperature of 1200°C is the highest combustion temperature available by our analytical facility. We usually repeat the combustion steps at 1200°C several times until the nitrogen release amounts drop to the 1200°C hot-blank level. The N_2/Ar ratios for the blanks were observed to be essentially the atmospheric ratio. See Ishida et al. (2012) and references therein for further procedural details and analytical performances. The nitrogen, carbon, and argon data in this article are the values subtracted for the hot- and cold-blank contributions. All error bars for the values denote 1σ errors.

Standard gas measurements were performed 21 times in total during the analytical session of the two Hayabusa2 samples. The reproducibility for the nitrogen isotope ratio during this session was 0.7‰ (1σ) for 60 picomoles of standard nitrogen gas. The standard gas was initially prepared from the ambient atmosphere, first sampled by a small vacuum component attached to the mass spectrometry line, followed by dilution. The standard gas is stored in a stainless-steel tank. A constant fraction of the standard gas is taken from the tank using a pipette volume between a set of two valves. We further calibrate the amount of 1 pipette of standard gas, and also the exact δ^{15}N value for the standard gas, by periodically measuring a solid working standard sample, a synthetic Fe_4N powder (Kojundo Chemical Laboratory). The nitrogen concentration and the δ^{15}N value of the Fe_4N powder are further calibrated using a dynamic-type elemental analyzer Flash2000 coupled via a ConFlo IV to a Delta V Advantage isotope ratio mass spectrometer (Thermo Fisher Scientific) at Tohoku University. The δ^{15}N values are calibrated with a commercial stable isotope standard of L-Alanine having $\delta^{15}N_{air} = 1.8 \pm 0.2$‰ (Shoko Science), which was calibrated against IAEA-N-1 and IAEA-N-2 with δ^{15}N values of +0.43‰ and +20.41‰, respectively.

A problem we recently recognized regards this cross-calibration procedure. The amount of nitrogen generated by a minimum weighable portion of Fe_4N is still too large for our static-type mass spectrometer, so that we normally perform multiple pressure reduction steps before introducing the gas to the mass spectrometer. A volume used for this pressure reduction was recently discovered to have been overestimated by about 10%. This error led to an overestimation of the nitrogen sensitivity for the mass spectrometer adopted by Okazaki, Marty, et al. (2022). The corrected nitrogen concentrations estimated for the two Ryugu samples, A0105-07 and C0106-07, given here correspond to 75% and 73%, respectively, of those reported in Okazaki, Marty, et al. (2022). The respective C/N ratios given here are 1.35 and 1.37 times higher, respectively.

RESULTS

The stepwise combustion results for the two Ryugu samples A0105-07 and C0106-07, as well as for Ivuna, are shown in Figures 1–3, respectively, and the isotope and concentration data are in Table S1. In Figures 1–3, the nitrogen release patterns and the nitrogen isotope ratios

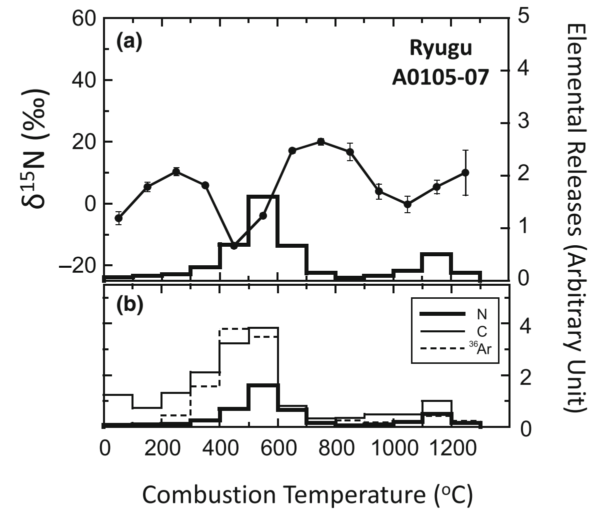

FIGURE 1. The stepwise combustion profile of the Ryugu return sample A0105-07. The δ^{15}N values and N amounts released at individual temperature steps are plotted in the upper panel (a), whereas the release amounts of C and ^{36}Ar are compared with the N amounts in the lower panel (b). The release amounts are plotted in arbitrary units. However, the areas for respective elements described by the bar graphs are designed to be proportional to the total amounts of the corresponding elements released from the three samples: Ryugu A0105-07 (Figure 1), Ryugu C0106-07 (Figure 2), and Ivuna (Figure 3). Error bars of the δ^{15}N values denote 1σ. Note that the data plotted beyond 1200°C are actually the second combustion step duplicated at 1200°C.

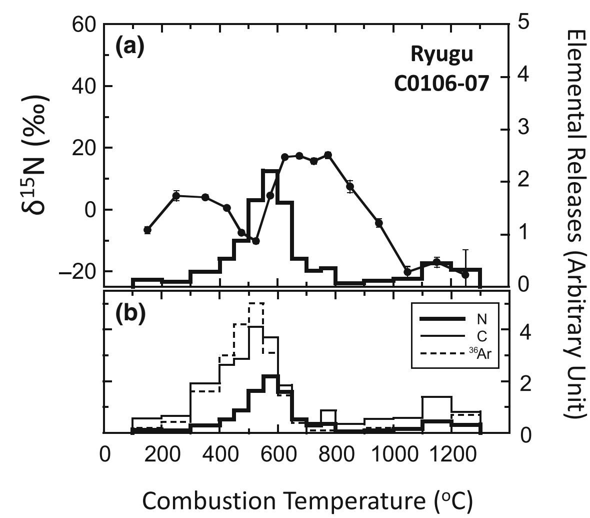

FIGURE 2. The stepwise combustion profile for the Ryugu return sample C0106-07. See the caption of Figure 1 for further notes.

are displayed in the upper panels (panel a), and the release patterns of carbon and ^{36}Ar, compared to those of nitrogen, are displayed in the lower panels (panel b). The release patterns are plotted in arbitrary units, although

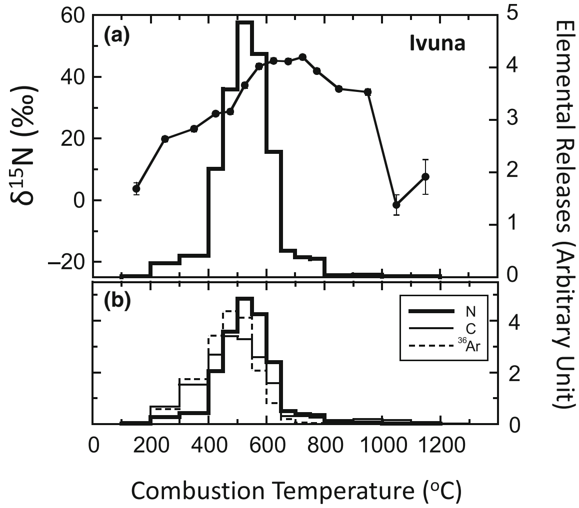

FIGURE 3. The stepwise combustion profile for Ivuna (CI). The release amounts are plotted in arbitrary units. For this sample, the areas for the three elements described by the bar graphs in panel b are designed to be the same. See the caption of Figure 1 for other notes.

the areas described by the bars are designed to scale the bulk concentrations for the three samples. Table 1 summarizes the bulk composition for the three samples, as well as for Y-980115 for comparison, analyzed by the same facility. Table 1 also shows the fractional compositions released at different temperature domains: low temperature (LT: $T \leq 600°C$), mid-temperature (MT: $600°C < T \leq 800°C$), and high temperature (HT: $800°C < T \leq 1200°C$). The stepwise combustion release profiles for the LT, MT, and HT fractions will be first discussed at the beginning of the following section.

DISCUSSION

Low-Temperature (LT, ≤600°C) Domain

The steps using the lowest combustion temperatures of 100 and 200°C tend to start with atmospheric or, more often, slightly negative $\delta^{15}N$ values. This tendency is common not only among the samples reported in this article but also for all samples, including terrestrial samples analyzed by the same facility and method (e.g., Pinti et al., 2001, 2009). We therefore infer that the negative $\delta^{15}N$ values at the lowest temperatures at least partly reflect isotope fractionation associated either with adsorption, release of adsorbed air, or with preferential release of ^{14}N by diffusion or other kinetic effects. Partial association with air adsorption is supported by the co-release of argon with a rather high $^{40}Ar/^{36}Ar$ ratio approaching the atmospheric ratio (296) (Table S1), which is much higher than the $^{40}Ar/^{36}Ar$ ratio for the primordial argon widely known to be much lower than unity (Ozima & Podosek, 2002). By assigning all ^{40}Ar released at this temperature domain to the atmospheric origin, we estimate the upper limit for the contribution of adsorbed air to the ^{36}Ar budget released in the LT domain to be 1%–2%. Also, for nitrogen, the release fraction of the first temperature step is always minor (0.2%–4%) compared to the subtotals for the LT domain. Whatever is the origin of this nitrogen component with negative or near-zero $\delta^{15}N$ values, we ignored this component in further discussions.

After the first release of the negative or near-zero $\delta^{15}N$ component, the $\delta^{15}N$ values remain below +40‰, the typical bulk $\delta^{15}N$ value observed among the CI falls. The two Ryugu samples never exhibit $\delta^{15}N$ values higher than +10‰ at this temperature domain, which is lower than Ivuna, which displays values between +20 and +30‰ at 300–500°C. A possible explanation for the lower $\delta^{15}N$ values, in principle, can be a contribution by terrestrial contamination. However, contamination that originates from atmospheric nitrogen is usually negligible. For instance, terrestrial rock samples with little indigenous nitrogen, prepared in the ambient atmosphere, often show bulk nitrogen concentrations as low as 0.1 ppm (e.g., Hashizume et al., 2016). Note that air is not the sole potential contamination source of nitrogen; for example, organic sources can often significantly contribute (e.g., Hashizume et al., 2016; Hashizume & Sugiura, 1995; Pinti et al., 2001, 2009). These sample surface-correlated organic sources are expected to be released at the temperature range in-between those of adsorbed air and organic matter, the latter being combusted typically at 400–600°C (e.g., Ishida et al., 2017). However, the Ryugu samples are treated carefully never to be in contact with terrestrial organic sources, or with natural atmosphere that could carry some organic compounds. Therefore, it is difficult to explain lower $\delta^{15}N$ values by larger contamination than Ivuna. We will revisit this issue later to demonstrate that the terrestrial contamination is not a major nitrogen source in the Ryugu samples.

Between 500 and 600°C, the major part of the organic nitrogen is released. Here, Ryugu samples and Ivuna showed further contrasting $\delta^{15}N$ values and nitrogen concentrations, which are also reflected in the bulk nitrogen compositions of these samples. While Ivuna released abundant nitrogen with positive $\delta^{15}N$ values approaching the typical bulk range for the CI falls, the amount of nitrogen released from the Ryugu samples was less than a half that of Ivuna, and associated with negative $\delta^{15}N$ values. One reason for this $\delta^{15}N$ dip is likely the combustion of presolar nanodiamonds that occurs at temperatures mainly around $500 \pm 50°C$ (Russell et al., 1996). However, as discussed later, nitrogen from

TABLE 1. Summary of bulk and temperature domain data reported in this study.

	Weight		N	$\delta^{15}N_{AIR}$			C	C/N		^{36}Ar	^{36}Ar/N	
	mg		ppmw	‰	err.	Corr.	ppmw	mol mol^{-1}	err	pmol g^{-1}	nmol mol^{-1}	err
Ryugu A0105-07	0.1180	Total	524	1.7	0.5	7	68,100	151	7	64.7	1730	140
		LT	308	−4.5	0.5	4	48,600	184	11	51.8	2360	120
		MT	91	17.7	0.6		5000	64	5	5.6	860	60
		HT	126	5.5	1.8	7	14,400	134	15	7.4	820	540
Ryugu C0106-07	0.1185	Total	617	0.2	0.6	5	63,900	121	4	68.7	1560	70
		LT	336	−1.6	0.4	6	39,900	139	6	54.1	2250	90
		MT	156	17.0	0.5		7900	60	3	5.9	530	30
		HT	125	−15.7	2.5	−14	16,100	150	11	8.7	980	260
Ivuna	0.75	Total	1113	36.4	0.4	39	43,100	45	2	55.6	350	10
		LT	898	34.5	0.5	38	35,300	46	2	51.7	400	20
		MT	202	45.0	0.6		5300	31	2	3.0	100	10
		HT	13	28.7	0.9	44	2600	225	22	0.9	480	320
Y-980115	0.92	Total	438	4.0	0.3		33,600	90	3	38.0	1220	40

Note: Subtotals for temperature (T) domains: LT: $T \leq 600°C$; MT: $600°C < T \leq 800°C$; HT: $800°C < T$. Corr: Rough estimates of non-presolar $\delta^{15}N$ values, corrected for N from nanodiamonds (LT) or SiC (HT). All errors are 1σ.

this presolar component cannot fully explain the contrasting $\delta^{15}N$ values observed between these samples. The $\delta^{15}N$ values for the organic nitrogen released at this temperature domain appear to be different between Ryugu and the CI falls.

Within the LT domain, the major release occurred not only for nitrogen but also for carbon and ^{36}Ar. The super-CI chondritic bulk concentrations of carbon and ^{36}Ar in the two Ryugu samples are reflected in the abundant releases of these two elements in this temperature domain. The release patterns of these two elements (Figures 1b, 2b, and 3b) are similar for Ryugu samples and Ivuna. Based on these release patterns, the major carrier phases of carbon and ^{36}Ar appear to be common in Ryugu samples and CI falls. While the release patterns for carbon and ^{36}Ar are similar between Ryugu samples and Ivuna, nitrogen exhibits marked relative depletions in the Ryugu samples compared to Ivuna. However, the release patterns for nitrogen are not particularly different between Ryugu samples and Ivuna. For instance, both Ryugu samples and Ivuna reach peak release of nitrogen at similar temperatures of 550–600°C. Another point in common is that the peak of nitrogen release occurs at a higher temperature than the peak of C release. If nitrogen is homogeneously contained in organic carbon, a concurrent release of both elements is expected. These observations suggest that the nitrogen carrier phase/site may not be the same as that for major portions of carbon or ^{36}Ar, but the main phases/sites are not necessarily different between Ryugu samples and Ivuna.

Mid-Temperature (MT, $600°C < T \leq 800°C$) Domain

In the MT domain, above 600°C up to 800°C, the amount of nitrogen released continues to decrease after the peak release at 550 or 600°C. Here, a $\delta^{15}N$ plateau, that is, similar $\delta^{15}N$ values over consecutive temperature steps, is observed. By the stepwise combustion method applied to bulk samples, which are often a mixture of several components with different $\delta^{15}N$ values trapped by different carriers, the $\delta^{15}N$ value observed at a given temperature step does not necessarily represent the true value for a particular endmember. Often, they exhibit intermediate and variable values in-between those of the endmembers co-released at this temperature. A plateau $\delta^{15}N$ value, on the other hand, can be interpreted to represent the true value for a pure endmember, with limited multi-component mixing taking place. From similar $\delta^{15}N$ values observed in four consecutive steps for Ryugu C0106-07, thus imply the presence of an endmember component with $\delta^{15}N = +17 \pm 1‰$ in this sample. The same component is probably also present in A0105-07, although the temperature step is too coarse to precisely recognize the plateau. In Ivuna, the same host phase, inferred from the identical release temperature range, possesses a different $\delta^{15}N$ value of $+45 \pm 1‰$. Note that a similar $\delta^{15}N$ plateau was observed for Orgueil at the corresponding temperature domain, with $\delta^{15}N$ values between +40‰ and +49‰ (Grady et al., 2002), which resembles the MT profile of Ivuna.

The C/N ratio for the MT domain of 64 ± 5 and 60 ± 3 observed for Ryugu A0105-07 and C0106-07, respectively, and 31 ± 2 for Ivuna, are lower than for the other temperature domains. This suggests that the phase responsible for the $\delta^{15}N$ plateau, if it is a carbonaceous phase, is relatively nitrogen-rich, up to 3× the bulk. The MT domain corresponds to the combustion temperature of graphite (Grady et al., 1986), as well as the decomposition temperature of carbonate (Boyd et al., 1997; Yokoyama et al., 2022). Although carbonates are abundantly present in CI chondrites, nitrogen is less likely to be released from the carbonates, since carbonates generally accommodate little nitrogen (Sephton et al., 2003). Graphite or related combustible-carbon phases could be a likely candidate for the host phase of the MT nitrogen. In this case, the C/N ratio for the nitrogen phase responsible at MT should be smaller than the measured values, because of the contribution from potentially N-free carbonates. According to Yokoyama et al. (2022), the carbonate-form inorganic carbon in Ryugu and Ivuna accounts for ~10% of the bulk carbon. Applying this proportion and assuming that the carbonate release by our analyses occurred totally within the MT domain, the carbonate-form carbon may contribute >80% of the total C release at MT, both from Ivuna and Ryugu. Therefore, the best estimate for the C/N ratio of the host phase for the MT nitrogen is estimated to be ~10 or lower.

High-Temperature (HT, >800°C) Domain

In the HT domain, above 800°C, minor fractions of nitrogen are released from Ryugu samples and Ivuna, although the proportions released at this temperature domain are significantly different. Nitrogen releases are as high as 126 ppm among Ryugu samples, which accounts for 20% – 24% of the bulk nitrogen, whereas only 1% is released from Ivuna at >800°C. The low N concentration released from Ivuna at such high temperatures compares well with a previous temperature profile of N release in Orgueil by Grady et al. (2002).

The two Ryugu samples and Ivuna commonly show lower δ^{15}N values at HT compared to the corresponding MT fractions. A possible explanation for the generally lower δ^{15}N values could be the contribution of presolar silicon carbides. The contribution of the nitrogen component hosted in presolar silicon carbides will be discussed later. The abundant and heterogeneous presence of fairly refractory nitrogen components, with δ^{15}N values as high as +7‰ or −14‰ depending on the samples, which are distinctly lower than the typical bulk compositions for CI falls, appears to be a unique feature of the Ryugu samples.

Minor Contribution of Presolar Nitrogen to Bulk Samples

CI chondrites are known to contain the highest bulk abundances of carbonaceous presolar grains among all chondritic groups. High concentrations of nitrogen, associated with exotic nitrogen isotope ratios, are well documented among the carbonaceous presolar grains, such as nanodiamonds and silicon carbides (Hoppe & Zinner, 2000; Russell et al., 1997). Here, the possible contributions of nitrogen components hosted by these two major carbonaceous presolar grains to the analytical results of bulk Ryugu samples are estimated.

Presolar nanodiamonds contain abundant nitrogen with strikingly negative δ^{15}N values down to −350‰ (Russell et al., 1996). Broadley et al. (2023) studied the noble gas isotope composition from He to Xe, as well as the nitrogen isotope composition for two Ryugu samples. They reported that the Ryugu sample A0105-05 showed a higher Xe_{HL} proportion in the bulk of Xe compared to the CI falls, suggesting a higher nanodiamond concentration in this sample. Xe_{HL} is the characteristic component carried by the presolar nanodiamonds, which can be measured to quantify the abundance of this carrier in the samples. Taking the Xe_{HL}/Xe ratio of 2.7% reported by Broadley et al. (2023), and comparing the Xe_{HL} concentration with the one estimated for bulk Orgueil (Huss & Lewis, 1995), the nanodiamond abundance in A0105-05 is estimated to be approximately 2.3× higher than in Orgueil. Since in this work we did not analyze xenon isotopes, the nanodiamond abundances in our particular Ryugu samples are unknown. We attempt here to roughly estimate the contributions of the ^{14}N-rich nitrogen in the nanodiamond to our nitrogen isotope data, assuming that the nanodiamond concentrations are the same between the Ryugu sample A0105-05 and our allocated samples A0105-07 and C0106-07. We further assumed that the Xe_{HL}/N abundance ratio of the nanodiamonds was the same between the Ryugu samples and Orgueil. Since the Xe_{HL} and nitrogen abundances, and the δ^{15}N value in the nanodiamonds from Orgueil are well known (Huss & Lewis, 1994; Russell et al., 1996), the nitrogen contribution from the presolar diamonds in the Ryugu samples is then estimated to be 8.7 ppm. This accounts for less than 3% of the nitrogen budgets released at LT from both of our Ryugu samples. The mean δ^{15}N values for LT after subtraction of the nanodiamond contribution are roughly estimated to be +4‰ for A0105-07, and +6‰ for C0106-07. The corresponding estimate for Ivuna, assuming the same nanodiamond abundance as Orgueil, is +38‰, which falls within the typical δ^{15}N range of around +40‰ for CI falls. The contrasting presolar nanodiamond-corrected δ^{15}N values between the two Ryugu samples and Ivuna suggest that the δ^{15}N value for the major portion of nitrogen released at this temperature domain is indeed different between Ryugu and the CI falls.

Silicon carbide is the second most abundant presolar grain in primitive meteorites after nanodiamonds. Silicon carbide is known to combust at 1000°C and above (Russell et al., 1991, 1997). Ryugu grains also contain presolar silicon carbides in similar abundances to CI falls (Barosch et al., 2022). Presolar silicon carbides are nitrogen-rich in bulk, with C/N ~30. Though presolar silicon carbide grains show huge grain-to-grain ^{15}N/^{14}N variations, the bulk silicon carbide composition appears to be ^{14}N-rich, representing the isotope composition of the mainstream silicon carbide grains, which make up ~93% of all grains (Hoppe & Zinner, 2000). For example, the peak $\delta^{15}N$ value observed by the stepwise combustion of presolar silicon carbides from Orgueil is −576.5‰ (Russell et al., 1991). Assuming the same silicon carbide abundance with Orgueil, which is estimated to be as high as 28.5 ppm (Davidson et al., 2014; Huss & Lewis, 1995), and also assuming a bulk C/N of ~30 and $\delta^{15}N = -576.5$‰ for silicon carbides (Russell et al., 1991, 1997), the reduction due to silicon carbide in the mean $\delta^{15}N$ value of the HT domain for Ivuna could be as large as 15‰, which may fully account for the $\delta^{15}N$ difference between the average MT and HT values for this meteorite. In contrast, the mean $\delta^{15}N$ values estimated for the Ryugu samples A0105-07 and C0106-07 are lowered by 1.2‰ at most, applying the silicon carbide concentration of 23 (+7/−6) ppm estimated on Ryugu samples (Barosch et al., 2022).

Bulk Nitrogen Isotope Compositions

The bulk nitrogen data among CI-related samples, including all literature data, are compared here. For the Ryugu samples, the bulk data for A0105-07 and C0106-07, along with those of A0105-05 and C0106-06 reported in detail by Broadley et al. (2023), were collectively reported in brief by Okazaki, Marty, et al. (2022). Note, however, that our concentration data for A0105-07 and C0106-07 were revised after the first publication due to a technical reason (see the above methodology section). Another set of Ryugu bulk data comes from the aggregate samples A0106 (Naraoka et al., 2023) and C0107 (Oba et al., 2023). The examination of A0106 was duplicated three times using different subsets of the sample. To compare with the Ryugu samples, the bulk data for CI falls, all literature data, and our data for Ivuna reported in this article are plotted in Figure 4. Another data set comes from the Antarctic meteorite Y-980115. The bulk nitrogen data for Y-980115 by Chan et al. (2016), as well as the one obtained in our laboratory, are included in the plot.

First, our data for Ivuna and Y-980115, plotted as large symbols in Figure 4, are compared with literature data. Our analysis of Ivuna shows a bulk $\delta^{15}N$ value of +36‰. This value fits within the bulk $\delta^{15}N$ range of +31 to +52‰, exhibited by the three CI falls. The bulk $\delta^{15}N$ value for Y-980115, significantly lower than those of CI falls, was fairly well reproduced by our analysis with +4‰, in close agreement with the corresponding value of −2.8‰ by Chan et al. (2016). The two nitrogen measurements for Y-980115 also agree that the bulk nitrogen concentration is lower than the typical

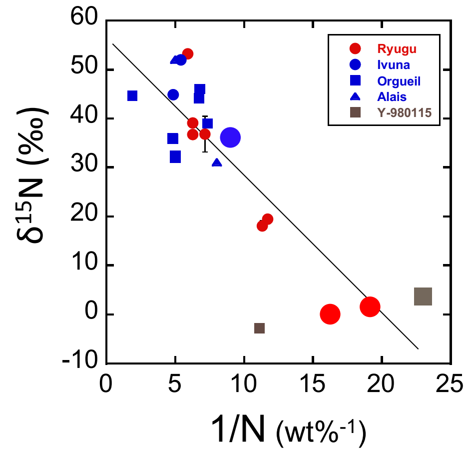

FIGURE 4. The bulk $\delta^{15}N$ values and N concentrations for Ryugu return samples, compared with CI-related meteorite data. Note that the inverse values of the N concentrations are plotted here to demonstrate a linear mixing relationship (see main text). Large symbols denote the data reported in this study, for the two Ryugu samples A0105-07 and C0106-07, Ivuna and Y-980115, to be compared with literature data in small symbols with the same shapes and colors. The 1σ-error bars attached to most symbols with the same colors, which denote analytical errors, were within the size of the symbols. The sole visible error bar in black color, attached to a particular Ryugu symbol, denotes the 1σ-deviation of independent results for three different batches of the same sample. The literature data for the corresponding meteorites are from Robert and Epstein (1982), Yang and Epstein (1983), Kerridge (1985), Grady et al. (2002), Pearson et al. (2006), Alexander et al. (2012), and Chan et al. (2016). The Ryugu return sample data are from Broadley et al. (2023), Naraoka et al. (2023), and Oba et al. (2023). The solid line represents the linear trend fitted to all data in this figure, expressed as follows: $\delta^{15}N$ (‰) = (56 ± 4)–(2.8 ± 0.4)/[N, wt%] ($r = -0.83$). (Color figure can be viewed at wileyonlinelibrary.com)

concentration range of 2100 ± 1100 ppm ($n = 11$) for CI falls. We report the nitrogen concentration of 438 ppm, which can be regarded as in agreement with 900 ppm reported by Chan et al. (2016), since a factor of two difference in the nitrogen concentrations is commonly observed among these carbonaceous meteorites. The overall agreement of our data with the literature values for the corresponding samples suggests that there are no serious analytical bias between the literature data and our data using the same analytical facility and protocols with those used to obtain our two Ryugu data.

Among the Ryugu samples, the bulk $\delta^{15}N$ values exhibit a large range from 0‰, observed in C0106-07, up to +53‰, observed in one of the bulk analyses for the aggregate sample A0106. Most importantly, the bulk $\delta^{15}N$ values are correlated with the nitrogen concentrations, with lower $\delta^{15}N$ values being found in samples with lower nitrogen concentrations. A0105-07 and C0106-07, reported in this article, showed the two lowest values both in $\delta^{15}N$ values and nitrogen concentrations. Corresponding values for A0105-05 and C0106-06, from Broadley et al. (2023), are higher compared to those for the abovementioned two samples, but are still significantly lower than those for the four Ryugu data from Naraoka et al. (2023) and Oba et al. (2023), which fit within the ranges exhibited by the CI falls. In Figure 4, where the horizontal axis is plotted as the inverse of the concentration, CI falls and the Antarctic CI chondrite plot on the same linear trend as the Ryugu samples. The linear regression line, fitted to all data for CI-related samples shown in Figure 4, is expressed as follows: δ^{15}N (‰) = (56 ± 4)–(2.8 ± 0.4)/[N, wt%] ($r = -0.83$). The linear trend in Figure 4 is explained by all samples containing a constant amount of one component with a low δ^{15}N value, which is mixed with variable amounts of a second component with a higher δ^{15}N value of +56 ± 4‰ that is given by the y-axis intercept of the best-fit line. If terrestrial contaminations were the second component, the intercept δ^{15}N value should come close to a value of zero, which is obviously not the case here. This clearly demonstrates that the near-zero bulk δ^{15}N values observed in our two Ryugu samples cannot be caused by the larger contributions of terrestrial contaminations. It is also highly unlikely to expect a constant contribution of terrestrial contaminations by as high as 500 ppm among all CI-related samples, given that the bulk nitrogen concentrations, including terrestrial contaminations, among terrestrial rocks often show bulk nitrogen concentrations as low as 0.1 ppm (e.g., Hashizume et al., 2016).

We can also rule out partial loss of nitrogen from a carrier by a Rayleigh-distillation type fractionation process in which the ^{14}N would be preferentially lost. In this case, we expect higher δ^{15}N values at lower nitrogen concentration, which is the opposite of what is observed.

Contributions of components with exotic isotope composition, such as the presolar grains, cosmogenic nuclides, or solar-wind component, are also unlikely to explain the difference in the bulk nitrogen abundances and isotope ratios. The minor contributions of ^{14}N-rich presolar nitrogen components have already been discussed. Given the cosmic ray exposure ages for the Ryugu A and C samples are 5.3 ± 0.9 Myr and 5.2 ± 0.8 Myr, respectively (Okazaki, Marty, et al., 2022), we can roughly estimate the cosmogenic-^{15}N contribution that could elevate the δ^{15}N values. Here, we tentatively applied the cosmogenic-^{15}N production rate obtained for L chondrites (Hashizume & Sugiura, 1995). This assumption is justified since cosmogenic-^{15}N is produced primarily from oxygen (Kung & Clayton, 1978), whose concentration is fairly constant among all chondrite classes. The increase in the δ^{15}N values due to the cosmogenic-^{15}N production is estimated to be as small as 0.05‰ for the HT fractions of our Ryugu samples, and much less for the corresponding bulk compositions. The heterogeneous distribution of the solar-wind nitrogen, with the δ^{15}N value as low as −400‰ (Marty et al., 2011), could in principle lead to variations in the bulk δ^{15}N values among Ryugu samples. Okazaki, Marty, et al. (2022) demonstrated that the solar-wind noble gas concentrations are different by several orders of magnitude among individual Ryugu samples. Among the examined samples, A0105-15 exhibited a prominently high solar-wind noble gas abundance, with the solar-wind ^{20}Ne concentration as high as 1.6×10^{-4} cm^{3}STP g^{-1}. We estimate that the solar-wind nitrogen concentrations among the Ryugu samples to be 0.1 ppm at most, applying the solar-wind abundance of A0105-15, and the solar ^{14}N/^{20}Ne ratio of 0.54 (Lodders, 2021). The extent of the bulk δ^{15}N values for Ryugu samples lowered by the solar-wind nitrogen is estimated to be negligibly small, as much as 0.1‰.

Two-Component Mixing of Nitrogen

The linear trend observed in Figure 4 can be interpreted within the framework of a two-component mixing, in which case the presence of at least two indigenous components is required among the CI-related samples. We tentatively designate these two components as A and B. Component A possesses a low δ^{15}N ≤0‰, while component B is ^{15}N-rich with a δ^{15}N of +56 ± 4‰, as shown by the δ^{15}N value of the linear trend extrapolated to the intercept for the vertical axis (Figure 4). The important distinction between these two components is that the component A must be roughly constant in its abundance among all samples, whereas the component B can vary sample-to-sample. The ^{15}N-poor and N-poor bulk properties of several samples, such as Ryugu A0105-05, A0105-07, C0106-06, C0106-07, and possibly Y-980115, are explained by the depletion of component B, whereas component A is present at the same abundance among all CI-related samples.

Here, we aim to further characterize the two nitrogen components. In Figure 5, the δ^{15}N values are plotted against the C/N ratios. All available bulk data for the CI-related samples are plotted here. In addition, the subtotal data distinguished by the combustion–temperature domains in the stepwise analyses are included, for Ryugu A0105-07 and C0106-07, and Ivuna (Table 1), and for Orgueil (Grady et al., 2002), although the HT data for Ivuna and Orgueil are omitted since these fractions are too minor. The bulk data overall exhibit a trend connecting a low C/N and high δ^{15}N end-composition, with a high C/N and low δ^{15}N end-composition.

It is worth noting that the temperature domain data for the abovementioned four samples are plotted along

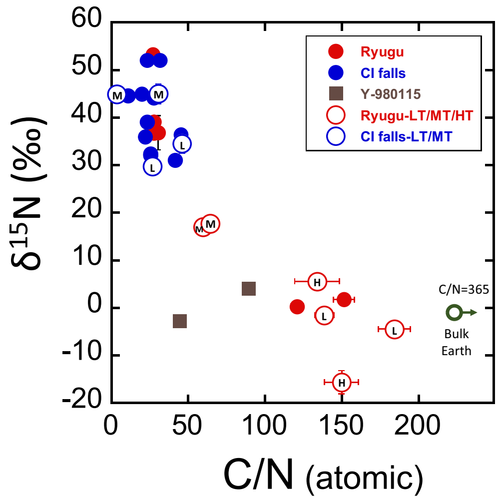

FIGURE 5. The $\delta^{15}N$ data for Ryugu return samples plotted against the C/N atomic ratios. Bulk data are plotted in solid symbols, whereas fractional data distinguished by the stepwise combustion analyses are plotted in open symbols, attached with labels that denote the temperature domains. L, M, and H, respectively, denote data for LT, MT, and HT domains (see main text). The notes on the error bars are the same as those in Figure 4. Bulk C and N concentrations and $\delta^{15}N$ data are from Yang and Epstein (1983), Kerridge (1985), Grady et al. (2002), Pearson et al. (2006), Alexander et al. (2012), Chan et al. (2016), and Naraoka et al. (2023), in addition to the data reported in this study. The bulk Earth composition is from Marty (2012). (Color figure can be viewed at wileyonlinelibrary.com)

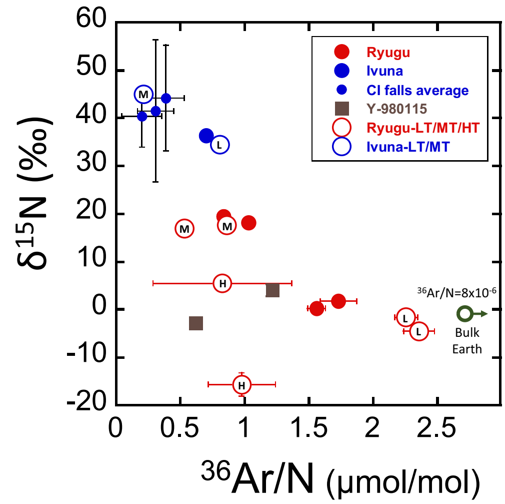

FIGURE 6. The $\delta^{15}N$ data for Ryugu return samples plotted against $^{36}Ar/N$ ratios. See the main text and caption of Figure 5 for further notes. Two of the four bulk Ryugu data are from Broadley et al. (2023). For comparison, averages of literature data for the three CI falls, Alais, Ivuna, and Orgueil, are plotted as small solid circles. Literature ^{36}Ar concentration data are from the data compilation by Schultz and Franke (2010). The bulk ^{36}Ar concentration data for Y-980115 are from King et al. (2019) and this study. The bulk Earth composition is from Marty (2012). (Color figure can be viewed at wileyonlinelibrary.com)

the trend exhibited by the bulk samples (Figure 5). Although the LT and HT fractions may contain more or less contributions from presolar grains, the corrections for the plotted $\delta^{15}N$ values are minor, as discussed above. There may exist a causal relationship between the different $\delta^{15}N$ values observed at different temperature domains. By applying the framework of the two-component mixing as we have proposed above to explain the bulk $\delta^{15}N$ differences among the CI-related samples, we can further explain the internal $\delta^{15}N$ differences within the samples by different mixing proportions of components A and B among different carrier phases. This may occur by redistribution of nitrogen components A and B through processing on the parent body, if these two components possessed different retentivities against the processing. For instance, upon a hypothesized processing of the starting organic matter, which contains both components A and B, the processed organic matter and the fluid may possess different proportions of components A and B. If the fluid was finally trapped in inclusions of secondary minerals such as carbonates, generated upon the parent body process, we would finally observe two nitrogen components with different $\delta^{15}N$ values released at different temperature steps.

The $\delta^{15}N$ values plotted against $^{36}Ar/N$ (Figure 6) display an overall similar trend to the one for the $\delta^{15}N$–C/N plot (Figure 5). This $\delta^{15}N$–$^{36}Ar/N$ trend could reflect the trend between $\delta^{15}N$ and C/N (Figure 5), combined with fairly proportional ^{36}Ar and C releases observed among samples and also between temperature domains (Figure S2). The data that deviate most from the trend in Figure 6 are the LT fractions of A0105-07 and C0106-07, which are shifted to the higher-$^{36}Ar/N$ direction. Dominant portions (79%–80%) of the ^{36}Ar from the bulk samples were released in these LT fractions. The argon, krypton, and xenon elemental compositions for Ryugu A0105-05 (Broadley et al., 2023) suggest that ^{36}Ar in this sample is dominated by the Q-phase noble gas (Ott, 2014). The abovementioned deviation of the $^{36}Ar/N$ ratios likely suggests that the Q-phase noble gas and the major portion of the LT nitrogen, though these two could be somewhat associated with carbon, are seemingly trapped in different phases/sites.

The Heterogeneous and Fragile ^{15}N-Rich Component—An Ammonia-Like Host Phase?

We proposed here a two-component mixing model for nitrogen among the CI-related samples, including the Ryugu samples, to explain the wide bulk $\delta^{15}N$ range that span between −3‰ and +53‰. The ^{15}N-rich isotope

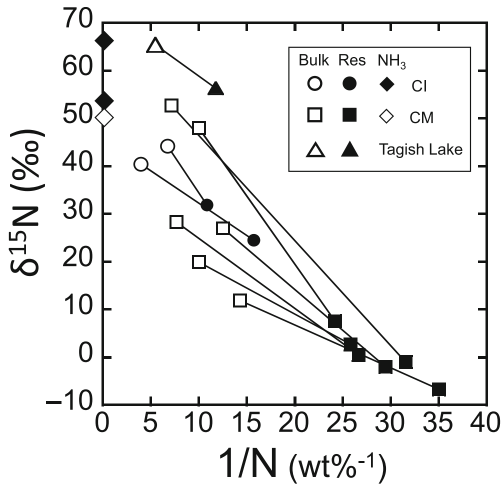

FIGURE 7. Bulk nitrogen isotope data compared with data of acid-treated residues for the corresponding samples. CI and CM chondrites, and Tagish Lake are plotted here. The bulk sample-based compositions for the residues are given by Alexander et al. (1998, 2007, 2014), estimated from the yields and the nitrogen concentrations of the acid residues. As for the CI bulk data, averages of all available data (Grady et al., 2002; Kerridge, 1985; Pearson et al., 2006; Robert & Epstein, 1982; Yang & Epstein, 1983; this study) are plotted as single symbols for Orgueil and Ivuna, respectively. Tagish Lake bulk data are the average of the data from Grady et al. (2002), Pearson et al. (2006), and Alexander et al. (2014). Bulk data for CM chondrites are from Pearson et al. (2006) and Alexander et al. (2012). The $\delta^{15}N$ data for ammonia evolved from Orgueil, Ivuna, and Murchison reported by Pizzarello and Williams (2012) are plotted on the *y*-intercept to demonstrate that the nitrogen component evolved to ammonia can be the likely candidate for the fragile component added to the CI chondrites (see main text).

signature was generally regarded as the typical characteristic for the CI chondrites, as well as for the other primitive carbonaceous chondrites, such as the CM group. However, the ^{15}N-rich component, in fact, may not always reside similarly among all these samples, but appears to be heterogeneously distributed sample-to-sample, and even among different nitrogen carrier phases that coexist in the bulk samples. The presence of a vulnerable ^{15}N-rich component in the Ryugu samples was also suggested by Broadley et al. (2023). This component in the CI-related samples likely possesses a $\delta^{15}N$ value of $+56 \pm 4$‰.

A depletion of the ^{15}N-rich component is known to occur upon chemical treatments of CI/CM chondrites (Alexander et al., 2007). Figure 7 compares the nitrogen isotope compositions of bulk carbonaceous chondrites with those of acid-treated residues for the corresponding meteorites. The residues systematically show lower $\delta^{15}N$ values and lower nitrogen concentrations, compared to the corresponding bulk meteorites. This suggests that, by the acid treatments, CI/CM chondrites lose a ^{15}N-rich component with a $\delta^{15}N$ value of $+50 \pm 30$‰, which is about the same as the one for component B proposed in our model. The component B could be chemically fragile compared to the component A. Alexander et al. (2015) proposed an alternative possibility to explain the N-depletion associated with the reduction of $\delta^{15}N$ values that occurred by the chemical treatment of CI/CM chondrites, which could be caused by the presence of fine-grained organics enriched in ^{15}N that are difficult to recover. In such a case, the 1/N–$\delta^{15}N$ correlations seen both among the bulk samples and also between bulk and insoluble organic matter (IOM) samples (Figure 4) must have actually occurred through different mechanisms.

The ^{15}N-rich component B has low C/N and $^{36}Ar/N$ ratios. That is to say, this nitrogen component can be relatively independent from other volatile elements, such as C or primordial noble gases. An interesting observation was provided by Pizzarello and Williams (2012), regarding the nitrogen chemical forms associated with the IOM in carbonaceous chondrites. Starting from the acid-IOM prepared from several chondrites, upon a hydrothermal treatment, they observed evolutions of ammonia molecules, which were enriched in ^{15}N. For the case of CI chondrites, the $\delta^{15}N$ values for ammonia released from Ivuna and Orgueil were estimated to be +66.4‰ and +53.4‰, respectively, which fits well with the $\delta^{15}N$ value for the component B estimated in this study. The identity of component B could be the ammonia originally bound to organic matter.

Nitrogen-bearing organic compounds and ammonium salts detected in CI-related samples (Chan et al., 2016; Glavin et al., 2018; Septhon, 2002), including the Ryugu samples (Naraoka et al., 2023; Oba et al., 2023; Parker et al., 2023; Yoshimura et al., 2023), are all attractive candidates to be assigned as the chemical forms of component B (or A) in meteorites (Figure S3). However, future works to elucidate the exact nature of components A or B will need to bear in mind that these components are required to be fairly abundant. According to the mixing diagrams in Figures 4 and 5, the nitrogen fraction of component B in CI falls or ^{15}N-rich Ryugu samples (A0106 or C0107) is required to be around two thirds of the bulk nitrogen in the samples, which roughly corresponds to nitrogen concentrations of 1000 ppm. The total concentrations of N-heterocyclic molecules detected in Ryugu or CI/CM samples appear to be several ppm at most (Oba et al., 2023), including the weight contributions from elements other than nitrogen. Even if we include nitrogen from other extractable organic compounds, such as amino acids and amines (Parker et al., 2023; see also reviews by Glavin et al., 2018; Septhon, 2002), the total nitrogen from these extractable compounds is insufficient to account for the required nitrogen concentration of component B.

Depletion of component B for part of the Ryugu samples, particularly in A0105-07 and C0106-07, could be due to "processing" experienced by these samples. This processing could have mimicked the effect of the hydrothermal treatment performed in the laboratory (Pizzarello & Williams, 2012), facilitating the detachment of ^{15}N-rich ammonia from organic matter. This situation appears to be the same as the case of the Antarctic meteorite Y-980115. In the case of Y-980115, we may infer that the processing could be related to the thermal metamorphism experienced by this sample (King et al., 2019), which possibly lead to the observed depletion of all volatile components, including the ^{15}N-rich nitrogen, primordial noble gases, and aqueous phases. However, for Ryugu A0105-07 and C0106-07, there is no evidence for the depletion of primordial noble gases in these samples. Nevertheless, this evidence may not be perfect, since nitrogen and primordial Q-phase noble gases seem to be trapped in different phases/sites and, therefore, could possess different retentivity to the processing. We defer the final interpretation for the exact processing histories for these Ryugu samples to future studies.

The possible relationship of components A and B with different δ^{15}N values caused by isotope exchange reactions anticipated during the aqueous alteration is evaluated here. For the moment, the equilibrium isotope exchange data for the exact target reactions, such as between organic nitrogen and ammonia molecules, are unknown. Here, we aim at making a qualitative evaluation referring to the fractionation model for terrestrial clay minerals, which involves equilibrium isotope exchange reactions associated with ammonia that possibly take place during the water–rock interaction (Haendel et al., 1986). Among natural clay minerals, where nitrogen is likely trapped as NH_4^+, the δ^{15}N values were observed to increase with decreasing nitrogen concentrations (Haendel et al., 1986). In their model, the enrichment of ^{15}N in trapped nitrogen (i.e., NH_4^+) was explained by an isotope exchange reaction; for instance,

$$^{15}NH_3 + {}^{14}NH_4^+ \leftrightarrow {}^{14}NH_3 + {}^{15}NH_4^+,$$

with the equilibrium isotope fractionation factors of, for example, 19‰ at 400 K or 27‰ at 300 K. Applying this exchange reaction on our isotope fractionation data, we expect a higher δ^{15}N for component A after the removal of the ammonia molecules, that is, component B, which is the opposite of the observed δ^{15}N relationship between these components.

Component B is distributed among several nitrogen carrier phases that appear to coexist in CI-related samples. It appears to be relatively concentrated in the nitrogen host phase released at MT. This could be due to the higher ammonia retentivity to this phase compared to the organic phase, which probably dominates the nitrogen release at LT. As discussed earlier, one of the possible candidates for the MT-host phase, inferred from the combustion temperature, is a graphite-like carbonaceous phase. However, it cannot be thermally processed organic matter. If so, the relative proportion of the fragile component B should be equal to or lower than the original organic phase. Probably there exists a minor but robust phase independent from the major organic phases, which better preserves nitrogen and possibly other volatile elements that accreted to the meteorite parent body, which is less affected by subsequent parent body processing.

The Ubiquitous and Robust ^{15}N-Poor Component

The counterpart nitrogen component to be mixed with the ^{15}N-rich nitrogen is relatively ^{15}N-poor, with the δ^{15}N value $\leq$0‰. As demonstrated in Figure 7, this ^{15}N-poor component resists acid treatments, along with IOM, which comprise the major portion of the organic matter contained in CI-related samples. Inferred also from the high C/N ratio estimated for the ^{15}N-poor component, this nitrogen component could be hosted by IOM. The presence of ^{15}N-depleted IOM in CI/CM chondrites is consistent with the conclusions by Alexander et al. (1998) and Sephton et al. (2003). Organic matter in CI-related samples was traditionally understood to be associated with ^{15}N-rich nitrogen, which is the dominant component observed in bulk CI falls. However, in this article, we propose that the bulk of the organic matter, or more precisely, of the organic carbon, is in fact, associated with ^{15}N-poor nitrogen, a component that could not be clearly confirmed by bulk analyses of CI falls. This component is probably also associated with the Q-phase noble gases. The ^{15}N-poor nitrogen and carbon in the IOM are possibly tightly bound, thus behave similarly stable against chemical treatments and potentially against parent body processes, thus are present ubiquitously among all CI-related samples at similar abundances.

The possible endmember δ^{15}N value for this component could even be negative. If we interpret the δ^{15}N values observed among the temperature domains strictly under the two-component mixing framework proposed here, this component may possess a δ^{15}N value as low as −16‰, which was observed at the HT fraction of Ryugu C0106-07. A fairly large amount of nitrogen was observed at this temperature domain; thus, it cannot be affected significantly by other minor components, such as presolar components. This $\delta^{15}N$ value comfortably fits within the bulk $\delta^{15}N$ range determined for the enstatite chondrites between −6‰ and −29‰ (Grady et al., 1986). The enstatite chondrites are one of the meteorite groups that potentially represent the material in the inner solar system, as suggested from similar O, Ti, Ca, and Mo isotopes with bulk Earth (e.g., Budde et al., 2019; Dauphas, 2017). This chondritic group is fairly enriched in volatile elements, including N (Grady et al., 1986), noble gases (Okazaki et al., 2010), and H (Piani et al., 2020), and thus can be regarded not only as rock-forming building blocks but also as one of the important sources of planetary volatiles. Assuming that the enstatite and CI chondrites represent the building blocks for the inner and outer solar systems, respectively, separated by the snowline, and with contrasting $\delta^{15}N$ values that bracket the terrestrial value of ~0‰ (e.g., Alexander et al., 2012; Marty, 2012; Hashizume, 2015), we propose here that both these meteorite groups may actually contain major nitrogen components with similar negative $\delta^{15}N$ values. The only distinction in terms of the nitrogen isotope systematics is that CI chondrites additionally contain a ^{15}N-rich fragile component.

^{15}N-Depleted Carbonaceous Asteroids as the Earth-Forming Building Blocks

The distribution of the ^{15}N-rich nitrogen source within the CI chondrite parent body(ies) cannot be clearly elucidated at this moment, since we do not yet know what kind of processing has mobilized this component. From looking at the Ryugu data, the ^{15}N-rich component appears to reside heterogeneously at the millimeter scale, that is, the grain-size scale. Ryugu A0106 and C0107 are aggregate samples that consist of numerous sub-mm grains (Naraoka et al., 2023; Oba et al., 2023). The ^{15}N-rich isotope signature observed for these samples may indicate that the bulk Ryugu parent body could be ^{15}N-enriched, akin to the CI falls. On the other hand, the other 4-mm-sized grain samples, A0105-05, A0105-07, C0106-06, and C0106-07, all showed a depletion in the ^{15}N-rich component, although to different extents. These observations are difficult to be reconciled with the abovementioned view of an "overall ^{15}N-rich" parent body. The heterogeneous distribution of N-containing organic molecules within a millimeter-sized Ryugu reported by Hashiguchi et al. (2023) could be somewhat related to the abovementioned millimeter-scale bulk nitrogen isotope heterogeneity. Prominent nitrogen isotope heterogeneity at the sub-micron scale is well known for the organic compounds in carbonaceous chondrites (e.g., Busemann et al., 2006; Hashizume et al., 2011), as well as for the Ryugu samples (Yabuta et al., 2023). However, the relationship between these small-scale isotope heterogeneities and the bulk nitrogen isotope heterogeneity observed here is not clear for the moment.

Although further studies are needed to resolve this issue, here, we would like to point out that the ^{15}N-depletion, if it was a parent body-wide phenomenon that characterize the bulk compositions of the whole carbonaceous asteroids, may give a large impact to the volatile supply models for Earth. As mentioned in the previous subsection, CI chondrites are considered to be one of the important sources of volatile elements to Earth. However, comparing the bulk compositions for the fall CI chondrites and the bulk silicate Earth, there are some large discrepancies. For instance, the C/N atomic ratio of bulk Earth is estimated to be 365 (Marty, 2012), whereas the corresponding ratio for the bulk CI falls ranges between 11 and 45 (Grady et al., 2002; Kerridge, 1985; Pearson et al., 2006; Yang & Epstein, 1983). This issue, so-called the missing nitrogen issue for the bulk Earth, is one of the critical problems that needs to be resolved to build a consistent volatile supply model for Earth. The volatile depletion on Earth is recognized distinguishably for nitrogen, against many other volatiles, including noble gases such as Ne and Ar (Marty, 2012), with lighter and heavier molecular weights compared to nitrogen. This observation rules out from the possibility that large-scale elemental fractionation occurred by molecular escape to space.

These issues could be resolved if the ^{15}N-depleted materials were the primary source of volatiles on Earth. The bulk C/N atomic ratio in one of the Ryugu samples exceeds 150, by which the discrepancy between the source and bulk Earth composition is greatly reduced. The much smaller discrepancy is also expected for the $^{36}Ar/N$ ratio. The Ryugu samples show bulk $^{36}Ar/N$ ratios up to 5× the corresponding ratio for Ivuna (Figure 6). Finally, the near-zero bulk $\delta^{15}N$ value, such as observed in Ryugu A0105-07 and C0106-07, could directly supply volatiles to Earth without the need of any isotope fractionation events that may have occurred on early Earth. This removes one of the obstacles to consider carbonaceous asteroids as a major volatile source for Earth. While marginally negative $\delta^{15}N$ values for Earth's building blocks, for example, enstatite chondrites or the potential ^{15}N-poor endmember in CI-related samples reported in this study, can be compensated for by a moderate ^{15}N-enrichment expected for atmospheric escape processes to space (Avice & Marty, 2020; Pepin, 1991). Conversely, a strong ^{15}N-depletion starting from source materials with distinctly positive $\delta^{15}N$ values could not occur by this process.

CONCLUSIONS

1. The nitrogen isotope compositions for two samples returned from the asteroid Ryugu were examined in detail using the stepwise combustion method. The two samples A0105-07 and C0106-07 showed bulk $\delta^{15}N$ values of $+1.7 \pm 0.5$ (1σ)‰ and $+0.2 \pm 0.6$‰, respectively. These values are significantly lower than the bulk $\delta^{15}N$ range between +31 and +52 reported for the three CI chondrites, Orgueil, Alais, and Ivuna, which show chemical compositions and textures similar to the Ryugu return samples.
2. Comparing the bulk nitrogen compositions among the CI-related samples, that is, all Ryugu samples examined so far at different laboratories, CI falls and Y-980115, a correlation was observed between the $\delta^{15}N$ values and nitrogen concentrations, with lower $\delta^{15}N$ associated with lower nitrogen concentrations. This trend can be explained by a two-component mixing model. One component possesses a $\delta^{15}N$ value of 0‰ or lower. This component appears to reside at a constant abundance among all CI-related samples. The other possesses a $\delta^{15}N$ value of $+56 \pm 4$‰. The abundance of this component varies on sample-by-sample basis. These two components appear to be characterized by different C/N ratios, the former with high C/N, as low as 184, and the latter with low C/N, which could even be C-free. The latter ^{15}N-rich component is possibly chemically fragile compared to the former one, which might have been often disturbed by parent body processes.
3. Nitrogen in Ryugu samples A0105-07 and C0106-07 appears to be hosted by several carriers with different $\delta^{15}N$ values, which span from −16‰ to +18‰, resolved by the combustion temperature. The different $\delta^{15}N$ values among different host phases can be explained by mixing of the abovementioned two components at different proportions. The difference in $\delta^{15}N$ values might have occurred because of the different retentivity of the ^{15}N-rich latter component among the nitrogen host phases.
4. Asteroid materials with a volatile composition similar to Ryugu A0105-07 and C0106-07, which possess higher C/N and $^{36}Ar/N$ ratios, and lower bulk $\delta^{15}N$ values, compared to the CI falls, can be an attractive candidate as one of the Earth-forming building blocks, which sourced the volatiles to Earth.

Acknowledgments—The Hayabusa2 mission was developed under the leadership of the Japan Aerospace Exploration Agency (JAXA). We are grateful to C. M. O'D Alexander, R. Wieler, and Editors I. Leya and A. J. T. Jull for their constructive reviews. Their comments greatly helped to improve the quality of the manuscript. This work was supported by JSPS KAKENHI Grant Number JP20H00190 to KH. The Antarctic meteorite was provided by the National Institute of Polar Research (NIPR) under the research program no. 1846.

Data Availability Statement—The data that support the findings of this study are available from the corresponding author upon reasonable request.

Editorial Handling—Dr. A. J. Timothy Jull

REFERENCES

Alexander, C. M. O'D. 2022. An Exploration of whether Earth Can be Built from Chondritic Components, Not Bulk Chondrites. *Geochimica et Cosmochimica Acta* 318: 428–451.

Alexander, C. M. O'D., Bowden, R., Fogel, M. L., and Howard, K. T. 2015. Carbonate Abundances and Isotopic Compositions in Chondrites. *Meteoritics & Planetary Science* 50: 810–833.

Alexander, C. M. O'D., Bowden, R., Fogel, M. L., Howard, K. T., Herd, C. D. K., and Nittler, L. R. 2012. The Provenances of Asteroids, and their Contributions to the Volatile Inventories of the Terrestrial Planets. *Science* 337: 721–23.

Alexander, C. M. O'D., Cody, G. D., Kebukawa, Y., Bowden, R., Fogel, M. L., Kilcoyne, A. L. D., Nittler, L. R., and Herd, C. D. K. 2014. Elemental, Isotopic, and Structural Changes in Tagish Lake Insoluble Organic Matter Produced by Parent Body Processes. *Meteoritics & Planetary Science* 49: 503–525.

Alexander, C. M. O'D., Fogel, M., Yabuta, H., and Cody, G. D. 2007. The Origin and Evolution of Chondrites Recorded in the Elemental and Isotopic Compositions of their Macromolecular Organic Matter. *Geochimica et Cosmochimica Acta* 71: 4380–4403.

Alexander, C. M. O'D., Russell, S. S., Arden, J. W., Ash, R. D., Grady, M. M., and Pillinger, C. T. 1998. The Origin of Chondritic Macromolecular Organic Matter: A Carbon and Nitrogen Isotope Study. *Meteoritics & Planetary Science* 33: 603–622.

Arakawa, M., Saiki, T., Wada, K., Ogawa, K., Kadono, T., Shirai, K., Sawada, H., et al. 2020. An Artificial Impact on the Asteroid (162173) Ryugu Formed a Crater in the Gravity-Dominated Regime. *Science* 368: 67–71.

Avice, G., and Marty, B. 2020. Perspectives on Atmospheric Evolution from Noble Gas and Nitrogen Isotopes on Earth, Mars & Venus. *Space Science Reviews* 216: 36.

Barosch, J., Nittler, L. R., Wang, J., Alexander, C. M. O'D., De Gregorio, B. T., Engrand, C., Kebukawa, Y., et al. 2022. Presolar Stardust in Asteroid Ryugu. *The Astrophysical Journal Letters* 935: L3 (12 pp).

Boyd, S., Wright, I. P., and Pillinger, C. T. 1997. Stepped-Heating of Carbonates and Carbon-Bearing Quartz Grains. *Chemical Geology* 134: 303–310.

Broadley, M. W., Byrne, D. J., Füri, E., Zimmermann, L., Marty, B., Okazaki, R., Yada, T., et al. 2023. The Noble

Gas and Nitrogen Relationship Between Ryugu and Carbonaceous Chondrites. *Geochimica et Cosmochimica Acta* 345: 62–74.
Budde, G., Burkhardt, C., and Kleine, T. 2019. Molybdenum Isotopic Evidence for the Late Accretion of Outer Solar System Material to Earth. *Nature Astronomy* 3: 736–741.
Busemann, H., Young, A. F., Alexander, C. M. O'D., Hoppe, P., Mukhopadhyay, S., and Nittler, L. R. 2006. Interstellar Chemistry Recorded in Organic Matter from Primitive Meteorites. *Science* 312: 727–730.
Chan, Q. H. S., Chikaraishi, Y., Takano, Y., Ogawa, N. O., and Ohkouchi, N. 2016. Amino Acid Compositions in Heated Carbonaceous Chondrites and their Compound-Specific Nitrogen Isotopic Ratios. *Earth, Planets and Space* 68: 7.
Dauphas, N. 2017. The Isotopic Nature of the Earth's Accreting Material through Time. *Nature* 541: 521–24.
Davidson, J., Busemann, H., Nittler, L. R., Alexander, C. M. O'D., Orthous-Daunay, F.-R., Franchi, I. A., and Hoppe, P. 2014. Abundances of Presolar Silicon Carbide Grains in Primitive Meteorites Determined by NanoSIMS. *Geochimica et Cosmochimica Acta* 139: 248–266.
Füri, E., and Marty, B. 2015. Nitrogen Isotope Variations in the Solar System. *Nature Geoscience* 8: 515–522.
Glavin, D. P., Alexander, C. M. D., Aponte, J. C., Dworkin, J. P., Elsila, J. E., and Yabuta, H. 2018. The Origin and Evolution of Organic Matter in Carbonaceous Chondrites and Links to their Parent Bodies. In *Primitive Meteorites and Asteroids*, edited by N. Abreu, 205–271. Amsterdam: Elsevier.
Grady, M. M., Verchovsky, A. B., Franchi, I. A., Wright, I. P., and Pillinger, C. T. 2002. Light Element Geochemistry of the Tagish Lake CI2 Chondrite: Comparison with CI1 and CM2 Meteorites. *Meteoritics & Planetary Science* 37: 713–735.
Grady, M. M., Wright, I. P., Carr, L. P., and Pillinger, C. T. 1986. Compositional Differences in Enstatite Chondrites Based on Carbon and Nitrogen Stable Isotope Measurements. *Geochimica et Cosmochimica Acta* 50: 2799–2813.
Haendel, D., Mühle, K., Nitzsche, H. M., Stiehl, G., and Wand, U. 1986. Isotopic Variations of the Fixed Nitrogen in Metamorphic Rocks. *Geochimica et Cosmochimica Acta* 50: 749–758.
Hashiguchi, M., Aoki, D., Fukushima, K., Naraoka, N., Takano, Y., Dworkin, J. P., Dworkin, K. E., et al. 2023. The Spatial Distribution of Soluble Organic Matter and its Relationship to Minerals in the Asteroid (162173) Ryugu. *Earth, Planets and Space* 75: 73. https://doi.org/10.1186/s40623-023-01792-w.
Hashizume, K. 2015. *Nitrogen Isotopes*. *Encyclopedia of Astrobiology*. Berlin Heidelberg: Springer-Verlag. https://doi.org/10.1007/978-3-642-27833-4_1065-3.
Hashizume, K., Pinti, D. L., Orberger, B., Cloquet, C., Jayananda, M., and Soyama, H. 2016. A Biological Switch at the Ocean Surface as a Cause of Laminations in a Precambrian Iron Formation. *Earth and Planetary Science Letters* 446: 27–36.
Hashizume, K., and Sugiura, N. 1995. Nitrogen Isotopes in Bulk Ordinary Chondrites. *Geochimica et Cosmochimica Acta* 59: 4057–69.
Hashizume, K., Takahata, N., Naraoka, H., and Sano, Y. 2011. Extreme Oxygen Isotope Anomaly with a Solar Origin Detected in Meteoritic Organics. *Nature Geoscience* 4: 165–68.
Hoppe, P., and Zinner, E. 2000. Presolar Dust Grains from Meteorites and their Stellar Sources. *Journal of Geophysical Research* 105: 10371–85.
Huss, G. R., and Lewis, R. S. 1994. Noble Gases in Presolar Diamonds I, Three Distinct Components and their Implications for Diamond Origins. *Meteoritics* 29: 791–810.
Huss, G. R., and Lewis, R. S. 1995. Presolar Diamond, SiC, and Graphite in Primitive Chondrites: Abundances as a Function of Meteorite Class and Petrologic Type. *Geochimica et Cosmochimica Acta* 59: 115–160.
Ishida, A., Hashizume, K., and Kakegawa, T. 2012. Stepwise Combustion Analyses of Distinct Nitrogen Isotopic Compositions on Paleoproterozoic Organic Matter. *Geochemical Journal* 46: 249–253.
Ishida, A., Hashizume, K., and Kakegawa, T. 2017. Microbial Nitrogen Cycle Enhanced by Continental Input Recorded in the Gunflint Formation. *Geochemical Perspectives Letters* 4: 13–18.
Ishida, A., Kitajima, K., Hashizume, K., Spicuzza, M. J., Zaitsev, A., Schulze, D. J., and Valley, J. W. 2023. Microscale Simultaneous Measurement of Carbon and Nitrogen Isotopes on Natural Diamond. *Geostandards and Geoanalytical Research* 47: 569–578. https://doi.org/10.1111/ggr.12485.
Kerridge, J. F. 1985. Carbon, Hydrogen and Nitrogen in Carbonaceous Chondrites: Abundances and Isotopic Compositions in Bulk Samples. *Geochimica et Cosmochimica Acta* 49: 1707–14.
King, A. J., Bates, H. C., Krietsch, D., Busemann, H., Clay, P. L., Schofield, P. F., and Russell, S. S. 2019. The Yamato-Type (CY) Carbonaceous Chondrite Group: Analogues for the Surface of Asteroid Ryugu? *Geochemistry* 79: 125531.
Kung, C. C., and Clayton, R. N. 1978. Nitrogen Abundances and Isotopic Compositions in Stony Meteorites. *Earth and Planetary Science Letters* 38: 421–435.
Lodders, K. 2021. Relative Atomic Solar System Abundances, Mass Fractions, and Atomic Masses of the Elements and their Isotopes, Composition of the Solar Photosphere, and Compositions of the Major Chondritic Meteorite Groups. *Space Science Reviews* 217: 44.
Marty, B. 2012. The Origins and Concentrations of Water, Carbon, Nitrogen and Noble Gases on Earth. *Earth and Planetary Science Letters* 313–314: 56–66.
Marty, B., Chaussidon, M., Wiens, R. C., Jurewicz, A. J. G., and Burnett, D. S. 2011. A ^{15}N-Poor Isotopic Composition for the Solar System as Shown by Genesis Solar Wind Samples. *Science* 332: 1533–36.
Morota, T., Sugita, S., Cho, Y., Kanamaru, M., Tatsumi, E., Sakatani, N., Honda, R., et al. 2020. Sample Collection from Asteroid (162173) Ryugu by Hayabusa2: Implications for Surface Evolution. *Science* 368: 654–59.
Nakamura, T., Matsumoto, M., Amano, K., Enokido, Y., Zolensky, M. E., Mikouchi, T., Genda, H., et al. 2022. Formation and Evolution of Carbonaceous Asteroid Ryugu: Direct Evidence from Returned Samples. *Science* 379: eabn8671. https://doi.org/10.1126/science.abn8671.
Naraoka, H., Takano, Y., Dworkin, J. P., Oba, Y., Hamase, K., Furusho, A., Ogawa, N. O., et al. 2023. Soluble Organic Molecules in Samples of the Carbonaceous

Asteroid (162173) Ryugu. *Science* 379: eabn9033. https://doi.org/10.1126/science.abn9033.

Oba, Y., Koga, T., Takano, Y., Ogawa, N. O., Ohkouchi, N., Sasaki, K., Sato, H., et al. 2023. Uracil in the Carbonaceous Asteroid (162173) Ryugu. *Nature Communications* 14: 1292. https://doi.org/10.1038/s41467-023-36904-3.

Okazaki, R., Marty, B., Busemann, H., Hashizume, K., Gilmour, J. D., Meshik, A., Yada, T., et al. 2022. Noble Gases and Nitrogen in Samples of Asteroid Ryugu Record its Volatile Sources and Recent Surface Evolution. *Science* 379: eabo0431. https://doi.org/10.1126/science.abo0431.

Okazaki, R., Takaoka, N., Nagao, K., and Nakamura, T. 2010. Noble Gases in Enstatite Chondrites Released by Stepped Crushing and Heating. *Meteoritics & Planetary Science* 45: 339–360.

Okazaki, R., Yamanouchi, S., Shimada, K., Baba, A., Kitajima, F., and Yada, T. 2022. Methods and Tools for Handling, Transportation, Weighing, and Pelletization Applied to the Initial Analysis of Volatile Components in the Hayabusa2 Samples. *Earth, Planets and Space* 74: 190.

Ott, U. 2014. Planetary and Pre-Solar Noble Gases in Meteorites. *Geochemistry* 74: 519–544.

Ozima, M., and Podosek, F. A. 2002. *Noble Gas Geochemistry*, 2nd ed. Cambridge: Cambridge University Press.

Parker, E. T., McLain, H. L., Glavin, D. P., Dworkin, J. P., Elsila, J. E., Aponte, J. C., Naraoka, H., et al. 2023. Extraterrestrial Amino Acids and Amines Identified in Asteroid Ryugu Samples Returned by the Hayabusa2 Mission. *Geochimica et Cosmochimica Acta* 347: 42–57.

Pearson, V. K., Sephton, M. A., Franchi, I. A., Gibson, J. M., and Gilmour, I. 2006. Carbon and Nitrogen in Carbonaceous Chondrites: Elemental Abundances and Stable Isotopic Compositions. *Meteoritics & Planetary Science* 41: 1899–1918.

Pepin, R. O. 1991. On the Origin and Early Evolution of Terrestrial Planetary Atmospheres and Meteoritic Volatiles. *Icarus* 92: 1–79.

Piani, L., Marrocchi, Y., Rigaudier, T., Vacher, L. G., Thomassin, D., and Marty, B. 2020. Earth's Water May Have Been Inherited from Material Similar to Enstatite Chondrite Meteorites. *Science* 369: 1110–13.

Pinti, D. L., Hashizume, K., and Matsuda, J. 2001. The Nitrogen and Argon Elemental and Isotopic Signature in >3.5 Ga Metasediments: Clues on the Chemical State of the Archean Ocean and the Deep Biosphere. *Geochimica et Cosmochimica Acta* 65: 2301–15.

Pinti, D. L., Hashizume, K., Sugihara, A., Massault, M., and Philippot, P. 2009. Isotopic Fractionation of Nitrogen and Carbon in Paleoarchean Cherts from Pilbara Craton, Western Australia: Origin of ^{15}N-Depleted Nitrogen. *Geochimica et Cosmochimica Acta* 73: 3819–48.

Pizzarello, S., and Williams, L. B. 2012. Ammonia in the Early Solar System: An Account from Carbonaceous Meteorites. *The Astrophysical Journal* 749: 161 (6 pp).

Robert, F., and Epstein, S. 1982. The Concentration and Isotopic Composition of Hydrogen, Carbon and Nitrogen in Carbonaceous Meteorites. *Geochimica et Cosmochimica Acta* 46: 81–95.

Russell, S. S., Arden, J. W., and Pillinger, C. T. 1996. A Carbon and Nitrogen Isotope Study of Diamond from Primitive Chondrites. *Meteoritics & Planetary Science* 31: 343–355.

Russell, S. S., Ash, R. D., Pillinger, C. T., and Arden, J. W. 1991. Meteoritic Silicon Carbide-Separate Grain Populations and Multiple Components Revealed by Stepped Combustion. *Meteoritics* 26: 390.

Russell, S. S., Ott, U., Alexander, C. M. O'D., Zinner, E. K., Arden, J. W., and Pillinger, C. T. 1997. Presolar Silicon Carbide from the Indarch (EH4) Meteorite: Comparison with Silicon Carbide Populations from Other Meteorite Classes. *Meteoritics & Planetary Science* 32: 719–732.

Saiki, T., Imamura, H., Arakawa, M., Wada, K., Takagi, Y., Hayakawa, M., Shirai, K., Yano, H., and Okamoto, C. 2017. The Small Carry-on Impactor (SCI) and the Hayabusa2 Impact Experiment. *Space Science Reviews* 208: 165–186.

Schultz, L., and Franke, L. 2010. Helium, Neon, and Argon in Meteorites: A Data Collection. *Meteoritics & Planetary Science* 39: 1889–90.

Sephton, M. A. 2002. Organic Compounds in Carbonaceous Meteorites. *Natural Product Reports* 19: 292–311.

Sephton, M. A., Verchovsky, A. B., Bland, P. A., Gilmour, J., Grady, M. M., and Wright, I. P. 2003. Investigating the Variations in Carbon and Nitrogen Isotopes in Carbonaceous Chondrites. *Geochimica et Cosmochimica Acta* 67: 2093–2108.

Tachibana, S., Sawada, H., Okazaki, R., Takano, Y., Sakamoto, K., Miura, Y. N., Okamoto, C., et al. 2022. Pebbles and Sand on Asteroid (162173) Ryugu: In Situ Observation and Particles Returned to Earth. *Science* 375: 1011–16.

Yabuta, H., Cody, G. D., Engrand, C., Kebukawa, Y., De Gregorio, B., Bonal, L., Remusat, L., et al. 2023. Macromolecular Organic Matter in Samples of the Asteroid (162173) Ryugu. *Science* 379: eabn9057. https://doi.org/10.1126/science.abn9057.

Yada, T., Abe, M., Okada, T., Nakato, A., Yogata, K., Miyazaki, A., Hatakeda, K., et al. 2022. Preliminary analysis of the Hayabusa2 Samples Returned from C-Type Asteroid Ryugu. *Nature Astronomy* 6: 214–220.

Yamamoto, T., Hashizume, K., Matsuda, J., and Kase, T. 1998. Distinct Indigenous Nitrogen Isotopic Components co-Existing in Ureilites. *Meteoritics & Planetary Science* 33: 857–870.

Yang, J., and Epstein, S. 1983. Interstellar Organic Matter in Meteorites. *Geochimica et Cosmochimica Acta* 47: 2199–2216.

Yokoyama, T., Nagashima, K., Nakai, I., Young, E. D., Abe, Y., Aléon, J., Alexander, C. M. O'D., et al. 2022. Samples Returned from the Asteroid Ryugu are Similar to Ivuna-Type Carbonaceous Meteorites. *Science* 379: eabn7850. https://doi.org/10.1126/science.abn7850.

Yoshimura, T., Takano, Y., Naraoka, H., Koga, T., Araoka, D., Ogawa, N. O., Schmitt-Kopplin, P., et al. 2023. Chemical Evolution of Primordial Salts and Organic Sulfur Molecules in the Asteroid 162173 Ryugu. *Nature Communications* 14: 5284 (11 pp).

SUPPORTING INFORMATION

Additional supporting information may be found in the online version of this article.

Data S1. List of the Hayabusa2-initial-analysis volatile team members.

Figure S1. Photographs of initial Ryugu samples and infrared reflectance spectra.

Figure S2. The ^{36}Ar abundances for Ryugu return samples plotted against the C abundances.

Figure S3. The representative nitrogen (N)-bearing molecules identified in the aggregate Ryugu samples for A0106 and C0107 by the sequential solvent extraction analysis (Naraoka et al. 2023; Oba et al., 2023; Parker et al., 2023).

Table S1. Stepwise combustion full data for Ryugu return sample: (a) A0105-07 and (b) C0106-07. (c) Stepwise combustion full data for Ivuna (CI).